

An Electronic Supplementary Information (ESI)

Preparation of double-layered nanosheets containing pH-responsive polymer networks in the interlayers and their conversion into single-layered nanosheets through cleavage of cross-linking points

Takuma Kamibe^a, Régis Guégan^b, Masashi Kunitake^c, Takehiko Tsukahara^d,

Naokazu Idota^{*d,e} and Yoshiyuki Sugahara^{*a,e}

^a Department of Applied Chemistry, School of Advanced Science and Engineering, Waseda University, 3-4-1 Okubo, Shinjuku-ku, Tokyo 169-8555

^b Global Center for Science and Engineering, Waseda University, 3-4-1 Okubo, Shinjuku-ku, Tokyo 169-8555, Japan

^c Institute of Industrial Nanomaterials, Kumamoto University, 2-39-1, Kurokami, Chuo-ku, Kumamoto 860-8555, Japan

^d Laboratory for Zero-Carbon Energy, Institute of Innovative Research, Tokyo Institute of Technology, 2-12-1-N1-6, Ookayama, Meguro-ku, Tokyo 152-8550, Japan

^e Kagami Memorial Research Institute for Materials Science and Technology, Waseda University, 2-8-26 Nishiwaseda, Shinjuku-ku, Tokyo 169-0051, Japan

***Corresponding Authors: idota.n.aa@m.titech.ac.jp, ys6546@waseda.jp**

Contents

Fig. S1 Schematic image of grafting reaction of hexaniobate with MEP and CPMP.	2
Fig. S2 XRD patterns of (a) $K_4Nb_6O_{17} \cdot 3H_2O$, (b) MEP_NbO, (c) $2C_{18}MeN_NbO$, (d) CPMP_NbO, (e) PNB_NbO with $FeK\alpha$ radiation and (f) PNB_NbO with $CuK\alpha$ radiation.	2
Fig. S3 Solid-state ^{31}P NMR spectra of (a) MEP_NbO and (b) CPMP_NbO.	3
Fig. S4 TG curves of CPMP_NbO and PNB_NbO.	3
Fig. S5 The expected hydrolysis of TBA_PNB@pH4_NbO.	4
Fig. S6 Photographs of colloidal dispersions with Tyndall scattering of (a) PNB@pH4_NbO, (b) TBA_PNB_NbO and (c) TBA_PNB@pH4_NbO, and TEM images and electron diffraction patterns of (d) PNB@pH4_NbO, (e) TBA_PNB_NbO and (f) TBA_PNB@pH4_NbO.	5
Fig. S7 The enlarged cross-section profiles of (a) PNB@pH4_NbO, (b) TBA_PNB_NbO and (c) TBA_PNB@pH4_NbO in Fig. 7 (a), Fig. 8 (a) and (c), respectively.	6

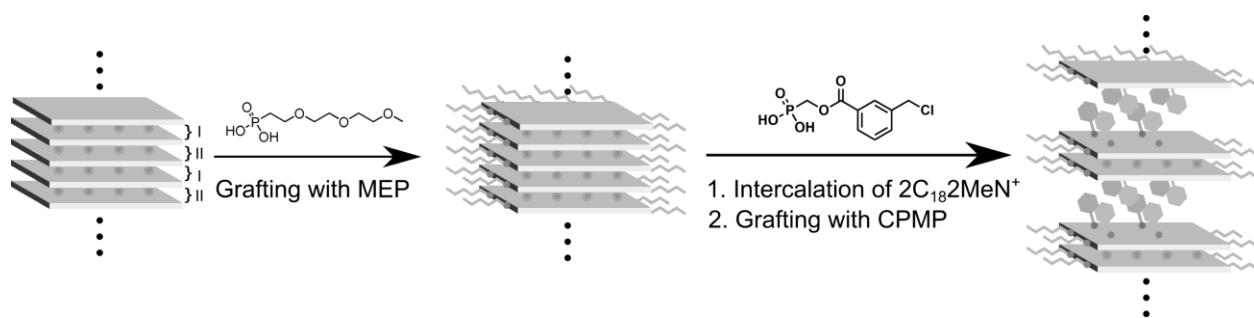


Fig. S1 Schematic image of grafting reaction of hexaniobate with MEP and CPMP.

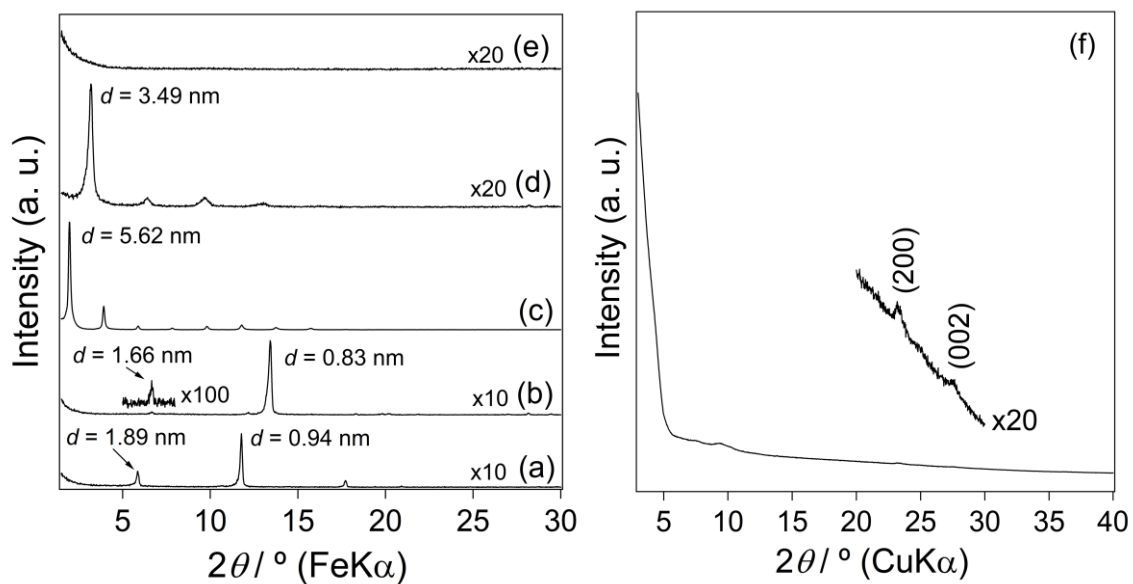


Fig. S2 XRD patterns of (a) $\text{K}_4\text{Nb}_6\text{O}_{17} \cdot 3\text{H}_2\text{O}$, (b) MEP_NbO, (c) $2\text{C}_{18}2\text{MeN}_\text{NbO}$, (d) CPMP_NbO, (e) PNB_NbO with FeK α radiation and (f) PNB_NbO with CuK α radiation.

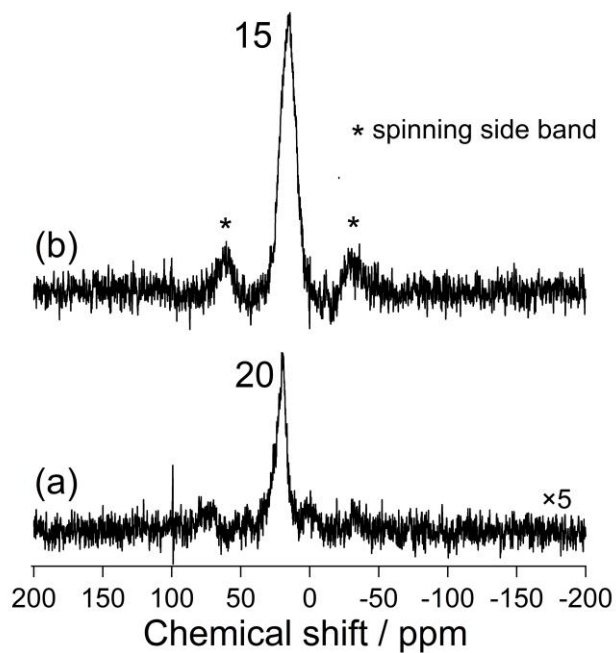


Fig. S3 Solid-state ^{31}P NMR spectra of (a) MEP_NbO and (b) CPMP_NbO.

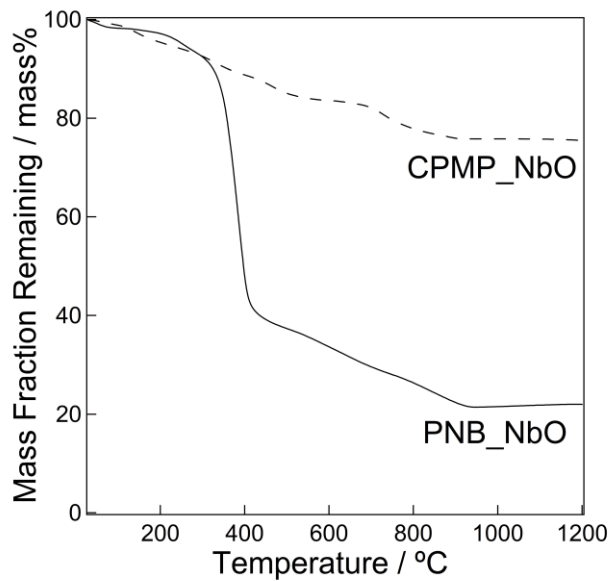


Fig. S4 TG curves of CPMP_NbO and PNB_NbO.

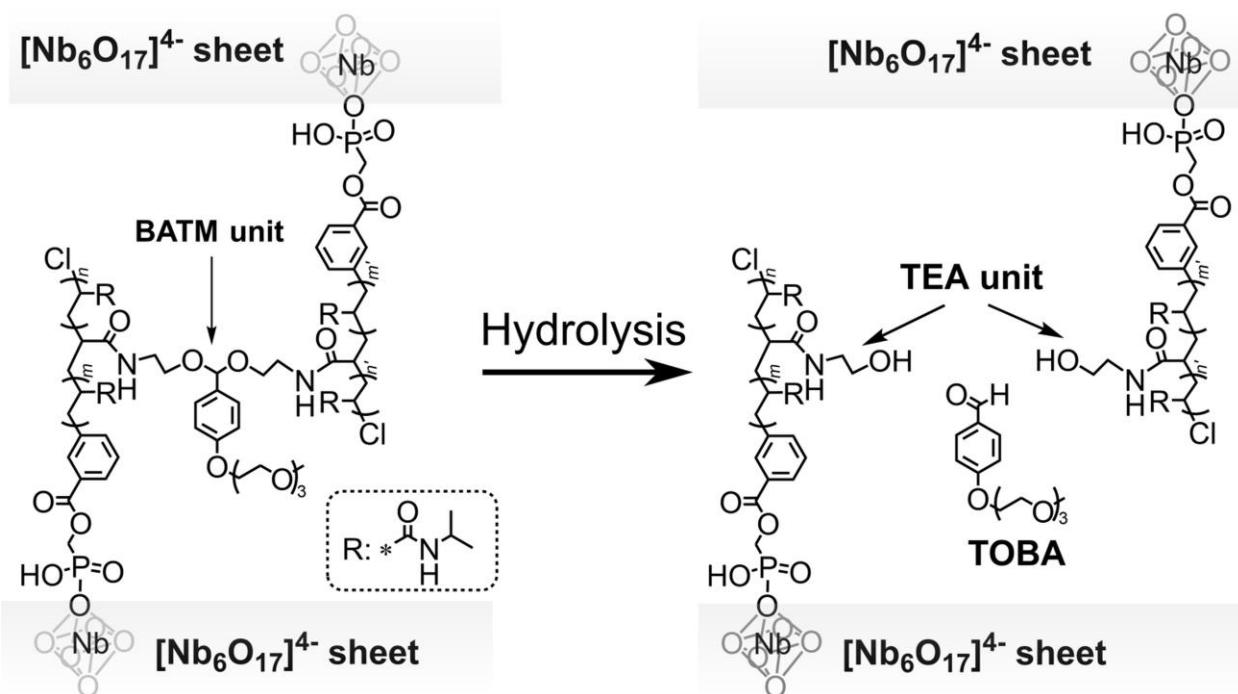


Fig. S5 The expected hydrolysis of TBA_PNB@pH4_NbO.

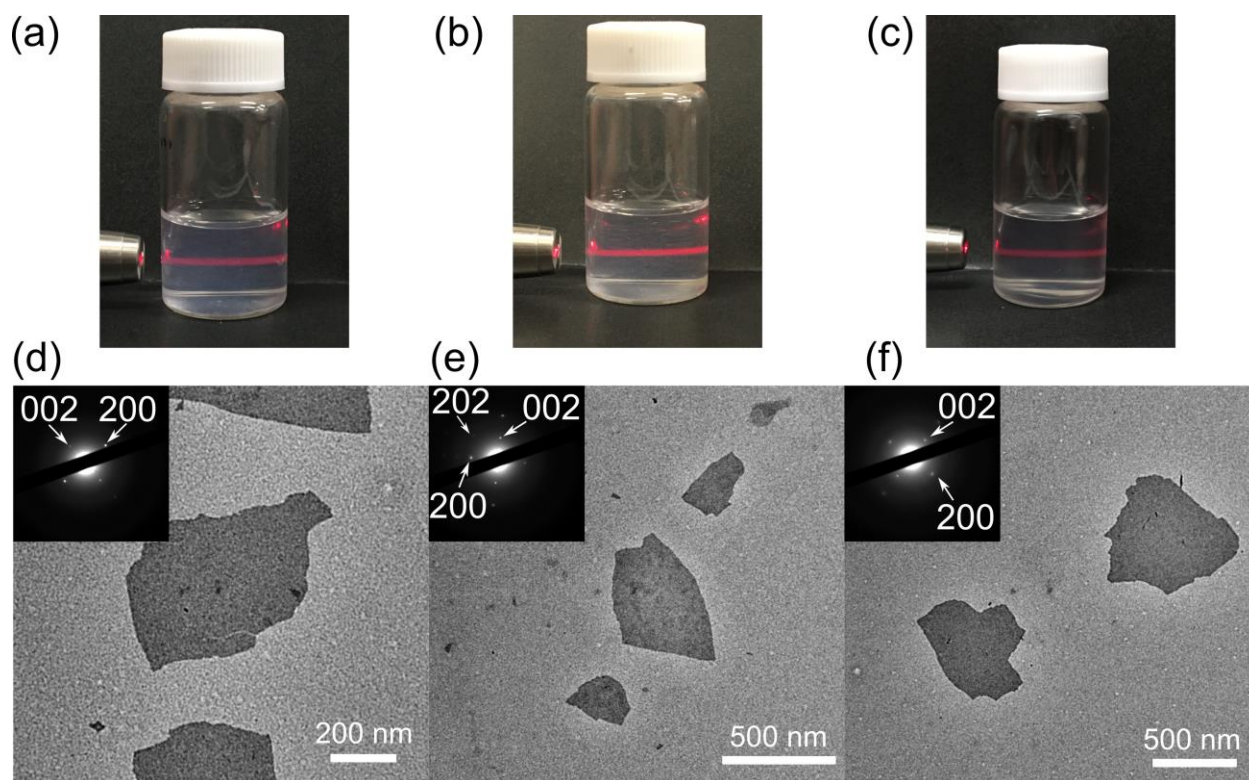


Fig. S6 Photographs of colloidal dispersions with Tyndall scattering of (a) PNB@pH4_NbO, (b) TBA_PNB_NbO and (c) TBA_PNB@pH4_NbO, and TEM images and electron diffraction patterns of (d) PNB@pH4_NbO, (e) TBA_PNB_NbO and (f) TBA_PNB@pH4_NbO.

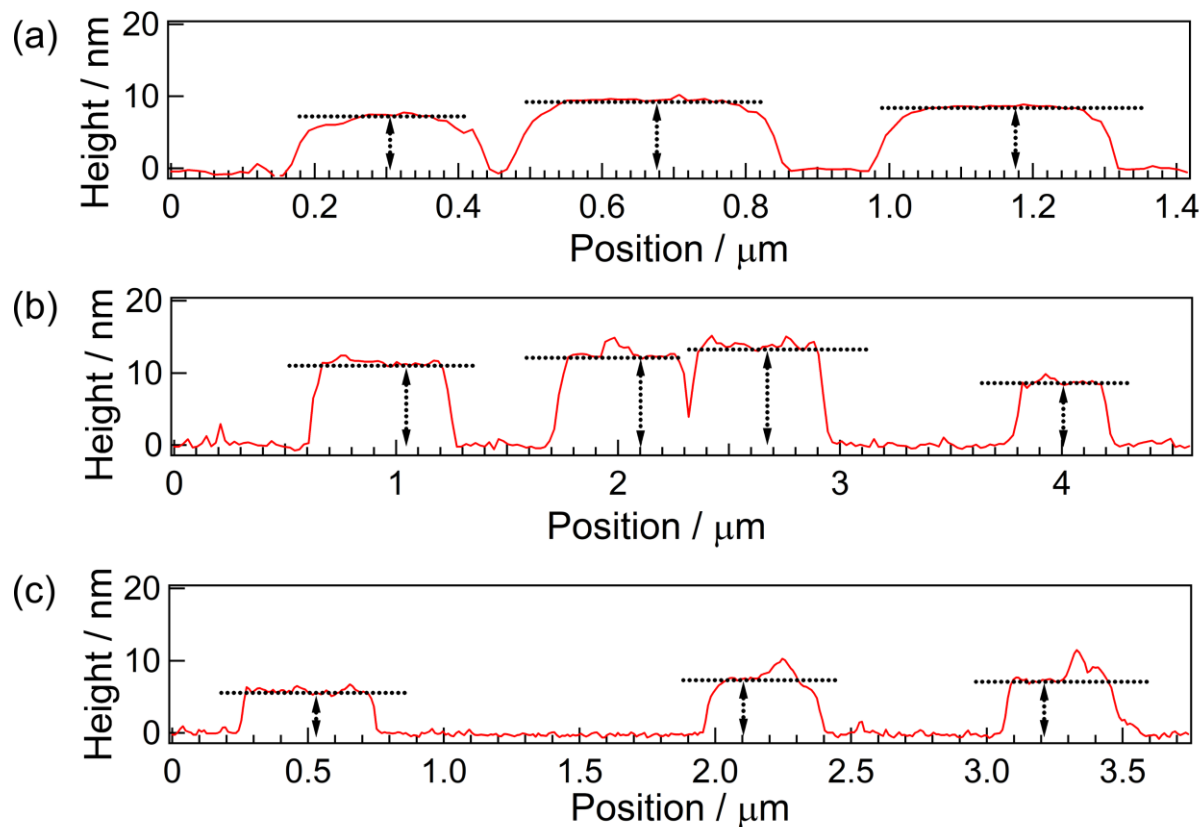


Fig. S7 The enlarged cross-section profiles of (a) PNB@pH4_NbO, (b) TBA_PNB_NbO and (c) TBA_PNB@pH4_NbO in Fig. 7 (a), Fig. 8 (a) and (c), respectively.